Numerical Simulation of Violent Free Surface through a Higher Order SPH Method

Zheng Xing [1] and Duan Wenyang[2]

[1] Deepwater Engineering Research Center, Harbin Engineering University, Room701, Ship&Ocean Building, No.145 Nantong Street, Harbin, China, 150001
E-mail: **zhengxing@hrbeu.edu.cn**

[2] Deepwater Engineering Research Center, Harbin Engineering University, Room302, Ship&Ocean Building, No.145 Nantong Street, Harbin, China, 150001
E-mail:**duanwenyang @hrbeu.edu.cn**

Abstract

A higher order smoothed particle hydrodynamics (SPH) is used to solve fluid flow problem with large free surface deformation. It is a meshless method and is used to solve the governing equations based on the Lagrangian description. Analysis has shown that the commonly used SPH method does not provide sufficient accuracy. The present paper has adopted an improved SPH method which provides a higher order accuracy. This is verified through a test case with non-uniform particle distribution in a rectangular domain. Simulation is then made for standing waves. Comparision is made with an analytical solution and agreement is good. Further simulation is made for the dam breaking problem.

Keywords: Smoothed Particle Hydrodynamics; Higher order accuracy; Free surface flow; Dam breaking

1 Introduction

Violent wave motion is a common phenomenon in marine and coastal engineering. When the wave encounters a structure in its path, very large impact can occur together with wave overturning, breaking and splashing. Current research into this kind of problem very much depends on laboratory experiment, which can be very expansive, time-consuming or even hazardous. The other important issue is of course the scaling effect. Numerical simulations have also been used for this type of problem, e.g., [1] [2] [3]. Although significant progress has been made, the success is still very much limited, especially to the cases where the free surface profile remains smooth. One of the reasons for this is that for the adopted mesh based method it is very difficult to generate a grid of high quality and high resolution for the overturning and breaking waves. The present paper investigates the potential of a non-mesh based method for the violent free surface.

Smoothed Particle Hydrodynamics (SPH) method is a meshless technique. It divides the fluid domain into a finite number of mass carrying particles. The movement of the particles and the pressure distribution in the fluid are obtained through solving the momentum equations and continuity equation within the Lagranian description of the motion. The method was first developed to simulate the evolution in astrophysics [4] [5], and was extended to free surface flow problem by Monaghan [6]. Because the path of each particle is tracked in SPH, the movement of particles can implicitly satisfy the kinematic condition on the free surface [7]. Because it does not require a mesh, it has the potential to deal with the complex free surface flows. Lo & Shao [8] used SPH method together with a large eddy simulation approach to simulate the near-shore solitary wave. Colagrossi & Landrini [9] applied SPH method to the two-dimensional interfacial flows. Souto et al [10] calculated the phase lag between the tank motion and the liquid response moment by SPH method. Furthermore sloshing moment amplitudes at a wide range of rolling frequencies were also obtained using SPH by Souto et al. [7].

However, being a relatively new comer, SPH still requires further refinement despite all the progress. For example, it is common to introduce an artificial term to correct the movement of the particle. This correction is non-physical. Its introduction is mainly to improve the stability of the scheme. Furthermore, the conventional low order SPH cannot provide results of high accuracy, especially in the area near the boundary of the fluid domain.

In this paper, the conventional SPH formulations are first introduced. Then a higher order smoothed particle hydrodynamics method is presented. A test case with a rectangular domain is chosen. When particles are distributed either uniformly or non-uniformly, the higher order SPH method is found to give more accurate results than conventional SPH method. The higher order SPH method is then used to simulate standing wave and dam breaking problem.

2 Conventional SPH formulations

The basic principle of SPH is that a function $f(\mathbf{x})$ and its spatial derivative can be approximated as

$$f(\mathbf{x}) = \int_{\Omega} f(\mathbf{x}')W(\mathbf{x}-\mathbf{x}',h)d\mathbf{x}' \tag{1}$$

$$\nabla f(\mathbf{x}) = \int_{\Omega} f(\mathbf{x}')\nabla W(\mathbf{x}-\mathbf{x}',h)d\mathbf{x}' \tag{2}$$

where h is the smoothed length, Ω is a support

domain enclosing point x, $W(\mathbf{x}-\mathbf{x}',h)$ is the kernel function which is zero on the boundary of Ω and satisfies $\int_\Omega W d\mathbf{x}' = 1$. If the kernel function is chosen as the Dirac δ-fucntion, these two equations become exact. Consider a small volume of $d\Omega$ of Ω. Assuming the mass of $d\Omega$ is m_j and the fluid density at the centre of $d\Omega$ is ρ_j, we then have $d\Omega = m_j / \rho_j$. Eqs. (1) and (2) can be written as

$$f(\mathbf{x}_i) = \sum_{j=1}^{N} \frac{m_j}{\rho_j} f(\mathbf{x}_j) W(x_i - x_j, h) \tag{3}$$

$$\nabla f(\mathbf{x}_j) = \sum_{j=1}^{N} \frac{m_j}{\rho_j} f(\mathbf{x}_j) \nabla_i W(\mathbf{x}_i - \mathbf{x}_j, h) \tag{4}$$

For the free surface flow problems, the discretised governing equations of SPH can be obtained from the continuity equation and momentum equations. If we ignore the viscosity, these equations can be written as

$$\frac{D\rho_i}{Dt} = \sum_{j=1}^{N} m_j V_{ij}^{\beta} \frac{\partial W_{ij}}{\partial x_i^{\beta}} \tag{6}$$

$$\frac{DV_i^{\alpha}}{Dt} = -\sum_{j=1}^{N} m_j \left(\frac{P_i}{\rho_i^2} + \frac{P_j}{\rho_j^2}\right) \frac{\partial W_{ij}}{\partial x_i^{\alpha}} + f_i^{\alpha} \tag{7}$$

where V^{α} is the velocity component in the direction of the x^{α} axis and $V_{ij}^{\beta} = V_i^{\beta} - V_j^{\beta}$, P is the pressure and f is the external volume force such as that due to gravity. When the velocity is obtained, the movement of the particle is obtained form

$$\frac{dx_i^{\alpha}}{dt} = v_i^{\alpha} - \varepsilon \sum_{j}^{N} \frac{m_j}{\rho_j} V_{ij}^{\alpha} W_{ij} \tag{8}$$

in which the second term on the right hand side is a correction term. ε in the equation is the velocity average correction coefficient, which is usually chosen between 0 and 1.

The relationship between pressure and density is assumed to be governed by the following equation

$$P = P_0\left(\left(\frac{\rho}{\rho_0}\right)^{\gamma} - 1\right) \tag{9}$$

where $P_0 = C_0^2 \rho_0 / \gamma$ and C_0 is the artificial sound speed. In the following calculations $\gamma = 7$ is taken and when the fluid is water, C_0 is taken as ten times maximum velocity.

3 A higher order SPH method

3.1 Accuracy analysis of conversional SPH method

To perform consistency analysis, it is quite illustrative to use a one dimensional problem. Assuming the length of the support domain is h and applying the Taylor expansion of $f(x)$ at the centre of the domain $x = x_0$, we can write Eq. (1) as

$$\begin{aligned} \int_\Omega f(x)W(x-x_0)dx &= \int_\Omega f(x_0)W(x-x_0)dx + \\ &\int_\Omega f'(x_0)(x-x_0)W(x-x_0)dx + O(h^2) \end{aligned} \tag{11}$$

in which W is of order $O(1/h)$ has been taken into account. Since $\int_\Omega W dx = 1$ and $\int_\Omega (x-x_0)W dx = 0$ if we assume that $W(x-x_0)$ is symmetric about x_0, Eq.(11) can be rewritten as

$$f(x_0) = \int_\Omega f(x) W dx + O(h^2) \tag{12}$$

Similarly, for the first order derivative, we have

$$\begin{aligned} \int_\Omega f(x)W_x dx &= f(x_0)\int_\Omega W_x dx + f'(x_0)\int_\Omega (x-x_0)W_x dx \\ &+ (f''(x_0)/2!)\int_\Omega (x-x_0)^2 W_x dx + O(h^2) \end{aligned} \tag{13}$$

in which $W_x = O(1/h^2)$ has been taken into account. If we notice $\int_\Omega W_x dx = 0$, $\int_\Omega (x-x_0)W_x dx = 1$, $\int_\Omega (x-x_0)^2 W_x dx = 0$, Eq.(13) can be rewritten as

$$f'(x_0) = \int_\Omega f(x) W_x dx + O(h^2) \tag{14}$$

For the second order derivative, we write

$$\begin{aligned} \int_\Omega f'(x)W_x dx &= f'(x_0)\int_\Omega W_x dx + f''(x_0)\int_\Omega (x-x_0)W_x dx \\ &+ (f'''(x_0)/2!)\int_\Omega (x-x_0)^2 W_x dx + O(h^2) \\ &= f''(x_0) + O(h^2) \end{aligned} \tag{15}$$

It may appear that Eqs.(12), (14) and (15) all give the second order accuracy. The fact is when Eq.(12) is used, the accuracy of $f(x_0)$ is order $O(h^2)$. When Eq.(12) is substituted into (14), we then have

$$\begin{aligned} f'(x_0) &= \int_\Omega [\int_\Omega f(x) W dx + O(h^2)] W_x dx + O(h^2) \\ &= \int_\Omega [\int_\Omega f(x) W dx] W_x dx + O(h) \end{aligned} \tag{16}$$

because $W_x = O(1/h^2)$. If we further substitute Eq.(16) into Eq.(15) and use the same argument, we find

$$f''(x_0) = \int_\Omega (\int_\Omega f(x) W_x dx) W_x dx + O(h^0) \tag{17}$$

This shows that in the conventional SPH method the error of the second order derivative does not decay with h. This is similar to what has been found in the conventional mesh based method [11].

3.2 Accuracy analysis of the higher order SPH

We can include the second order derivative in Eq.(12).

This gives

$$f(x_0)=\int_\Omega f(x)Wdx+\frac{1}{2}f''(x_0)\int_\Omega (x-x_0)^2Wdx+O(h^3) \tag{18}$$

If substitute Eq.(18) into Eq.(16), it can be easily seen the order of accuracy becomes $O(h^2)$. Subsequently, the order of accuracy of Eq.(17) becomes $O(h)$. This is consistent with what has been found in the mesh based method (Wu & Hu 2007a)

We now use a test case to verify the above derivation. A square domain with $0\le x\le 1,\ \ 0\le y\le 1$ is chosen. Within this domain we define a function $f(x,y)=x^2+y^2+2xy$, and then apply both the conventional and the high order SPH methods. We first write the Taylor expansion of $f(x,y)$ at the point (x_i,y_j) as

$$f(x,y)=f_{ij}+(x-x_i)f_{ijx}+(y-y_j)f_{ijy}+\frac{(x-x_i)^2}{2!}f_{ijxx} \tag{19}$$
$$+(x-x_i)(y-y_j)f_{ijxy}+\frac{(y-y_i)^2}{2!}f_{ijyy}+O(h^3)$$

where the subscripts i and j indicate location and the subscripts x and y indicate the derivatives. Multiplying both sides of Eq.(19) by W, W_x, W_y, W_{xx}, W_{xy}, W_{yy} repsectively, and integrating the results over the support domain Ω, we can get

$$\begin{aligned}\int_\Omega f(x,y)W_k ds &= f_{ij}\int_\Omega W_k ds+f_{ijx}\int_\Omega (x-x_i)W_k ds\\ &+f_{ijy}\int_\Omega (y-y_j)W_k ds+\frac{f_{ijxx}}{2!}\int_\Omega (x-x_i)^2W_k ds\\ &+\frac{f_{ijxy}}{2!}\int_\Omega (x-x_i)(y-y_j)W_k ds\\ &+\frac{f_{ijyy}}{2!}\int_\Omega (y-y_{ij})^2W_k ds+O(h^m),\end{aligned} \tag{20}$$

where $k=1\cdots 6$ $W_1=W$, $W_2=W_x$, $W_3=W_y$, $W_4=W_{xx}{}^2$, $W_5=W_{xy}$, $W_6=W_{yy}$, and $m=3$ if $k=1$, $m=2$ if $k=2,3$ and $m=1$, if $k=4,5,6$. We can substitute the expression of f into the left hand of Eq.(20) and perform all the integration. The result gives a 6×6 matrix equation which can be solved to obtain f_{ij}, f_{ijx}, f_{ijy}, f_{ixx}, f_{ixy}, f_{iyy}. Non-uniform particle distribution is used as shown in Fig.1. Fig.2 is a reproduction of Fig.1 but with ghost points denoted by hollow dots. The relative accuracy of the function and its derivatives from the conventional SPH method is shown in Fig.3 to 8. Very large error can be observed. When the higher order SPH method is used, the average of the relative errors corresponding to Figs.3-8 is shown in Fig.9 and is found to be negligible. This clearly shows the advantage of the higher order SPH method. More details of the results and analysis can be found in Zheng & Duan [12].

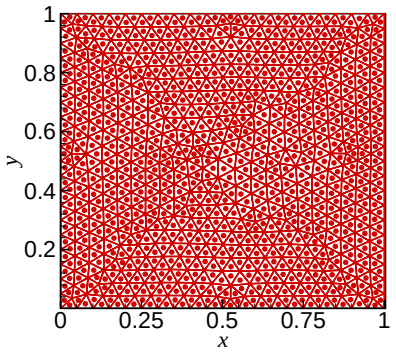

Figure1: Non-uniform particles in the domain

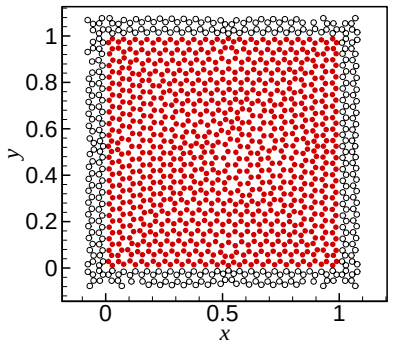

Fig.2 Non-uniform particle distribution with ghost points

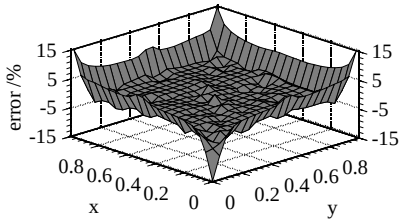

Fig.3 Error distribution of f

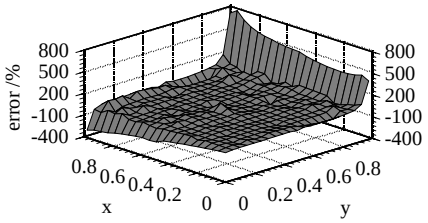

Fig.4 Error distribution of $\partial f/\partial x$

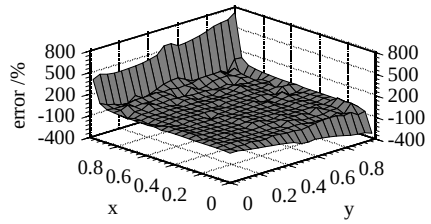

Fig.5 Error distribution of $\partial f/\partial y$

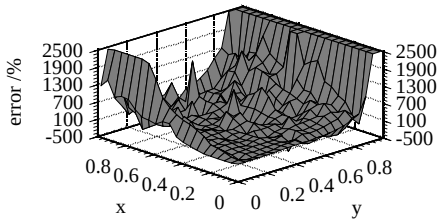

Fig.6 Error distribution of $\partial^2 f/\partial x^2$

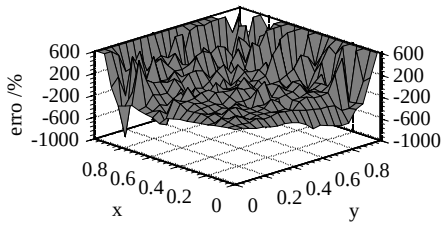

Fig.7 Error distribution of $\partial^2 f/(\partial x \partial y)$

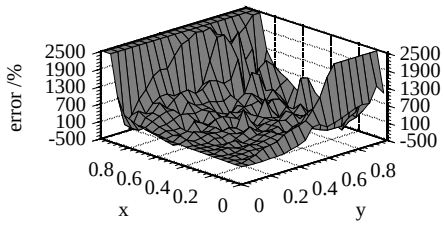

Fig.8 Error distribution of $\partial^2 f/\partial y^2$

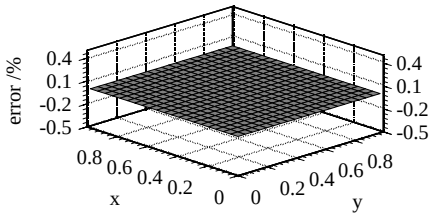

Fig.9 Average of errors by high order SPH

4 Numerical results

4.1 Standing wave

Based on the incompressible and inviscid theory, the velocity potential of the linear standing wave can be written as

$$\phi = \frac{a\omega}{k\sinh kd}\sin kx\cosh k(y+d)\cos\omega t \tag{21}$$

where a is the wave amplitude, k is the wave number which is related to the frequency through $\omega^2 = gk\tanh kd$, d is the water depth. The corresponding wave elevation then becomes

$$\eta = a\sin kx\sin\omega t \tag{22}$$

The velocity field and pressure distribution can be obtained as

$$u = \phi_x = \frac{a\omega}{\sinh kd}\cos kx\cosh k(y+d)\cos\omega t \tag{23}$$

$$v = \phi_y = \frac{a\omega}{\sinh kd}\sin kx\sinh k(y+d)\cos\omega t \tag{24}$$

$$\begin{aligned} P &= -\rho(\phi_t + gy) \\ &= \rho[\frac{a\omega^2}{k\sinh kd}\sin kx\cosh k(y+d)\sin\omega t - gy] \end{aligned} \tag{25}$$

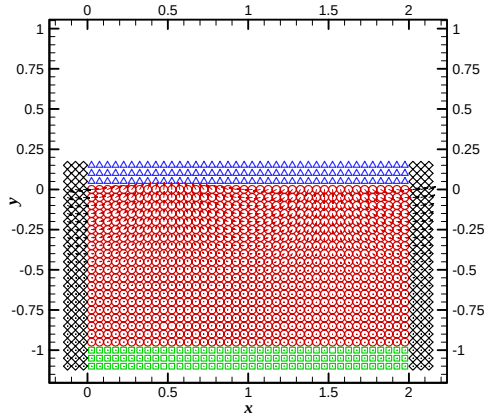

Fig.10 Particle distribution at initial time

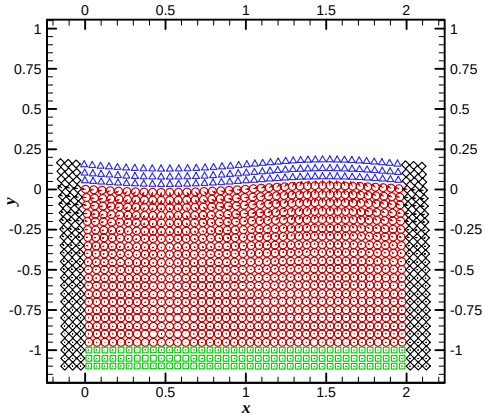

Fig.11 Particle distribution at 0.75s

In the SPH simulation, the initial wave elevation is taken as $\eta = 0$, and the initial velocity field is determined by Eq.(23) and (24). We then consider a case with water depth $d = 0.5$ m, wave length $\lambda = 2\pi / k = 2.0$ m and $a = 0.025m$. 800 particles are used in fluid domain. The initial particle distribution is shown in Fig.10. The circles are fluid particles, the squares, deltas and diamonds are ghost particles below the bottom, above the free surface and beyond the periodic boundaries respectively. The position of each particle is located at the centre of each symbol. Arrows represent the velocity direction. The ghost particles are redistributed at each time step and Fig.11 shows the particle distribution at 0.75s.

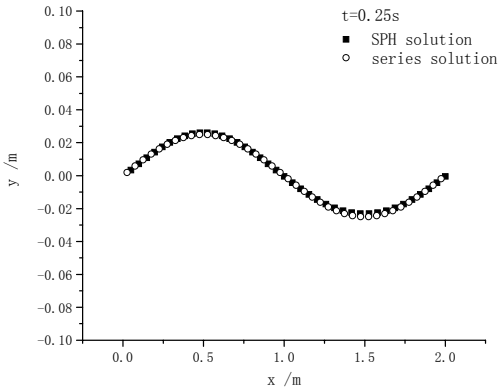

Fig12. Standing wave profile at t=0.25s

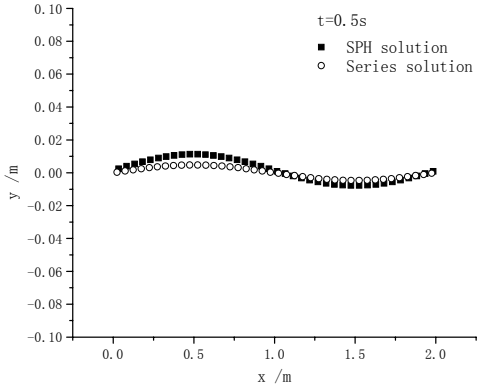

Fig13. Standing wave profile at t=0. 50s

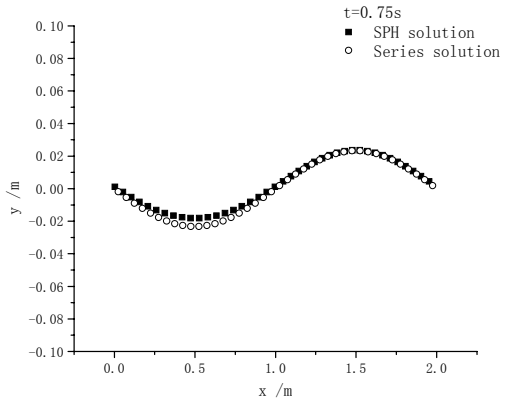

Fig14. Standing wave profile at t=0.75s

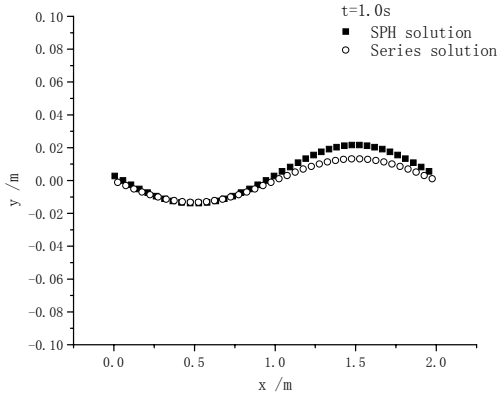

Fig15. Standing wave profile at t=1. 00s

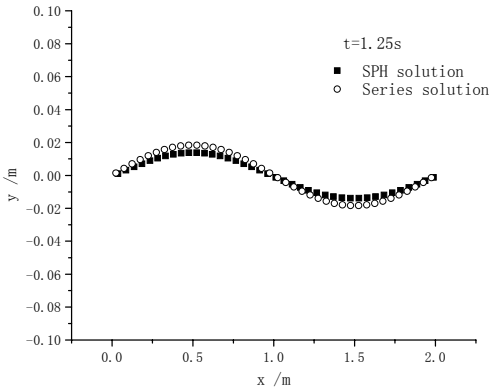

Fig16. Standing wave profile at t= 1.25s

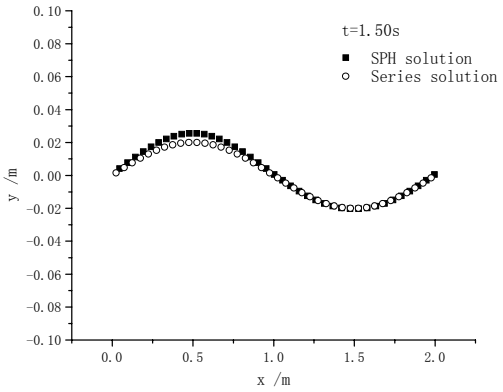

Fig17. Standing wave profile at t=1. 5s

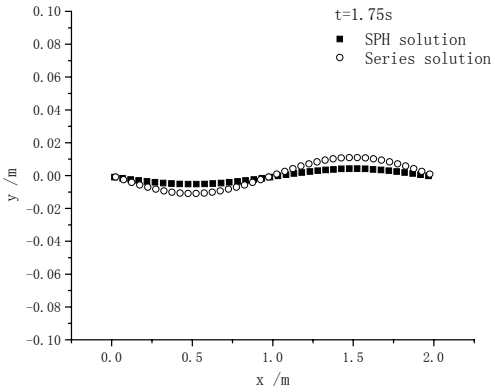

Fig18. Standing wave profile at t=1.75s

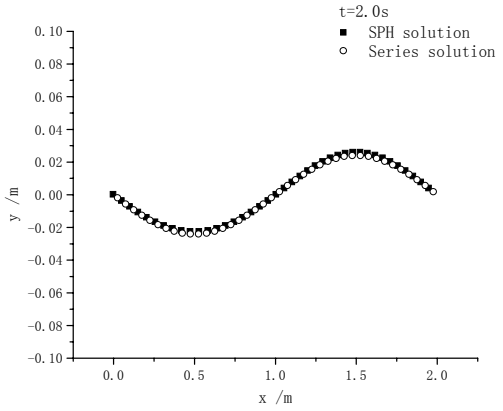

Fig19. Standing wave profile at t=2.0s

The results of standing wave simulation are shown as Fig.12~Fig.19 after every $0.25s$. Hollow dots are from the linear analytical solution, and solid dots are from the SPH simulation. The phase of wave elevation is very similar from the two methods. The results are in good agreement over all. There exist some differences between maximum wave crest and trough. Part of the reason is the SPH result is fully nonlinear while the analytical solution is linear. For the standing wave, the linear wave elevation can be completely flat or zero. When this happens, a small wave elevation can make big relative error. This explains the rather large difference in Fig.18.

4.2 Dam breaking

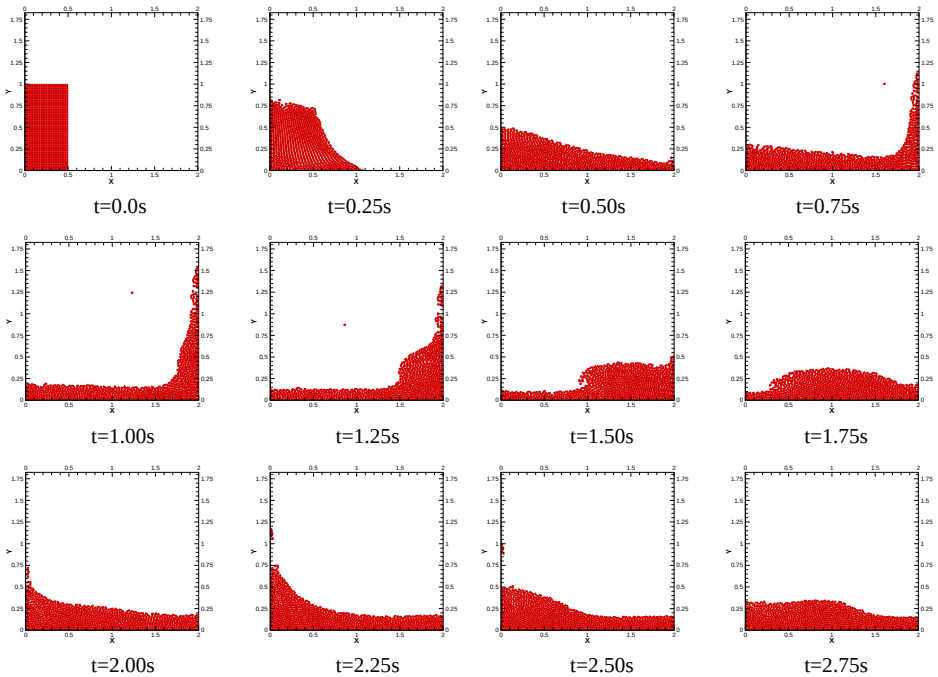

Fig.20 Numerical simulation process of dam breaking

Dam breaking is a widely used example in numerical simulations of free surface flow. In the case considered here, the height of initial water column is 1.0m and the width is 0.5m. A solid wall is placed at distance of 2.0m away from the dam. 1250 free fluid particles are used. The time step is taken as 10^{-4} s. Snapshots at different time steps of the numerical simulation are shown in Fig.20. It provides the process of water first moving towards the solid wall. After the collision it will move back and sloshing motion then starts.

5 Conclusions

In this paper, the foundation of traditional SPH method is introduced first, and then the accuracy analysis of kernel approximation is given, which demonstrates the low accuracy of traditional method, especially on the boundary domain. The improved method of traditional, C2SPH method is presented. According to the numerical test in rectangle area with particle non-uniform distribution, C2SPH can get high accuracy results, especially on the boundary domain. Simulation of standing wave is introduced to verify the improved of the new method, although there are some small differences between linear series solution and high order SPH solution. Finally, dam breaking is given to verify the advantage of SPH for violent free surface flow simulation.

Reference

[1] G.X. Wu (2006) “Fluid/structure impact”, Lecture notes, College of Shipbuilding Engineering, Harbin Engineering University, Harbin 150001, China

[2] G.X. Wu (2007a) “Fluid impact on a solid boundary”, *J. Fluids & Structures* Vol.23,pp755-765

[3] G.X. Wu (2007b) “Two dimensional liquid column and liquid droplet impact on a solid wedge” *Quat. J. of Mech. and Appl. Math.,* (*accepted*)

[4] Gingold R A, Monaghan J J. (1977) “Smoothed particle hydrodynamics: theory and application to non-spherical stars”. *Mon. Not. Roy. Astrou. Soc*., 181:pp375-389.

[5] Lucy L B. (1977) “A numerical approach to the testing of the fission hypothesis” *The Astron. J*., 82 (12):pp1013-1024.

[6] Monaghan J J. (1994) “Simulating free surface flows with SPH ”. *J. Computational Physics*, pp399-406.

[7] Souto I.A., Delorme L., Pe rez Rojas L., Abril S.P. (2006) “Liquid moment amplitude assessment in sloshing type problems with Smooth Paritcle Hydro dynamics”. *Ocean Engineering*, 33:pp1462-1484

[8] Y.M.Lo E., Shao S.D. (2002) “Simulation of near-shore solitary wave mechanics by an incompressible SPH method”. *Applied Ocean Research*, 24:pp275-286

[9] Colagrossi A., Landrini M. (2003) “Numerical simulation of interfacial flow by Smoothed Particle Hydrodynamics”. *J. Computational Physics.*, 191:pp448-475

[10] Souto I.A., Pe rez Rojas, L., Zamora, R. (2004) “Simulation of anti-roll tanks and sloshing type problems with smoothed particle hydrodynamics”. *Ocean Engineering,* 31:pp1169~1192

[11] G.X. Wu and Z.Z. Hu (2007) “A Taylor series based finite volume method the Navier-Stokes equations”, *Submitted for publication*

[12] X Zheng. and W.Y. Duan (2007) “An investigation on the accuracy analysis of second order consistency (C2SPH) method”, *Submitted for publication*